PCL SHAPE MEMORY POLYMER SCAFFOLDS PREPARED WITH VARIABLE CROSS-LINK DENSITY

An Undergraduate Research Scholars Thesis

by

VANESSA MARIE PAGE

Submitted to the Undergraduate Research Scholars program at
Texas A&M University
in partial fulfillment of the requirements for the designation as an

UNDERGRADUATE RESEARCH SCHOLAR

Approved by Research Advisor: Dr. Melissa Grunlan

May 2017

Major: Biomedical Engineering

TABLE OF CONTENTS

ABSTRACT

PCL Shape Memory Polymer Scaffolds Prepared with Variable Cross-Link Density

Vanessa Marie Page
Department of Biomedical Engineering
Texas A&M University

Research Advisor: Dr. Melissa Grunlan
Department of Biomedical Engineering, Department of Materials Science and Engineering
Texas A&M University

Poly(ε-caprolactone) (PCL) has been previously studied as a thermoresponsive shape memory polymer (SMP) for numerous biomedical applications due to its biocompatibility and biodegradability. We have previously investigated "self-fitting" porous scaffolds of cross-linked PCL-diacrylate (PCL-DA) that exhibited properties suitable for craniomaxillofacial (CMF) defect repair. Herein, in order to broaden scaffold mechanical properties and degradation profiles, the scaffold cross-link density was systematically varied by tuning PCL-DA macromer degree of polymerization (*n*). A broad range of PCL-DA degrees of polymerization (*n = 20, 40, 60* and *70*) were synthesized and prepared as porous scaffolds. The percent acrylation of the PCL-DA macromers was confirmed to ensure sufficient cross-linking. The impact of PCL-DA scaffold cross-link density on thermal properties (e.g. crystallinity), mechanical properties (e.g. stiffness and strength), *in vitro* degradation rate, and % porosity was determined.

DEDICATION

I would like to dedicate this thesis to Dr. Robin Page for instilling an appreciation for the inherent value of research for the global betterment of patient care at a young age.

ACKNOWLEDGEMENTS

I would like to thank my Faculty Advisor, Professor Grunlan, for her continually patient mentorship and guidance. I would also like to thank Lindsay Woodard, my graduate student research mentor, for her support and guidance throughout the course of this research.

CHAPTER I

INTRODUCTION

The objective of this research is to investigate the effect of cross-link density on the mechanical properties and degradation rate of porous shape memory polymer (SMP) scaffolds prepared from poly(ε-caprolactone) diacrylate (PCL-DA). These properties are essential towards advancing their utility as "self-fitting" scaffolds to treat irregularly shaped craniomaxillofacial (CMF) defects. PCL-DA macromer degree of polymerization (*n*), and, thus, cross-link density, was systematically varied *(n = 20, 40, 60* and *70*) to tune material properties (**Figure 1**).

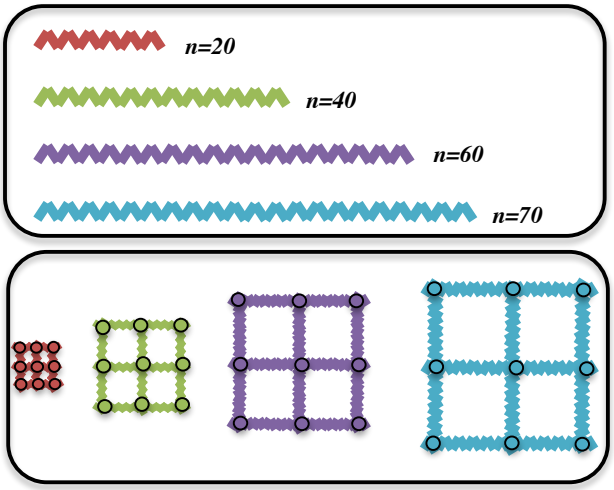

Figure 1. Schematic illustrating how macromer degree of polymerization *(n)* impacts cross-link density.

Clinical Application

CMF bones determine the primary shape of head, provide protection to intracranial tissues and functionality to surrounding soft tissues. CMF defects can be congenital or a result of injury and represent a significant clinical need. In the United States, approximately 96,000 CMF bone

defects are treated every year with an estimated cost of more than $1 billion.[3] In 2001, nearly 38,000 children underwent surgery to repair birth defects and close to 25,000 patients required maxillofacial surgery for injuries to the face and jaw.[4] Treatment of CMF defects remains a serious surgical challenge due to the critical need to fully restore function while simultaneously allowing aesthetic reparation.

While autografting is currently the gold standard, it is associated with donor site morbidity, resorption, and a lack of osseointegration due to an inability to tightly fit the graft within an often irregularly shaped defect.[5] Bone screws and bone plates can be utilized to provide additional fixity for the bone-to-graft union, but can cause further issues such as stress shielding, corrosion, and patient discomfort, often requiring an additional surgery for removal.[6] Xenografts have also been considered, but significant challenges with host immune response remain a challenge.

Shape Memory Polymers

The proposed scaffolds derive their self-fitting behavior due to their shape memory nature. SMPs are a class of polymers with continuously growing interest from the scientific community with an expansive range of potential applications, including self-expanding drug delivery stents[7], biodegradable minimally invasive surgical implants[8], and sails for aerospace applications.[2] SMPs are stimuli-responsive materials whose shapes can be modulated by the application of heat,[9-11] light,[12-13] magnetic field[14] or other environmental triggers such as the change of pH and the use of organic solvents.[13] Notably, SMPs have the potential to aid in development of "minimally invasive" implantable or surgical devices. Thus, a relatively bulky device fabricated from an SMP can be introduced *in vivo* in a temporary collapsed shape and subsequently expanded to its

permanent shape when thermally triggered.[9] Novel SMPs with the necessary properties could greatly expand their utilities in new applications that further impact quality of patient care.

Thermoresponsive SMPs are characterized by their ability to undergo shape change in response to temperature change (**Figure 2**). The shape change is made possible by "switching segments", crystalline (T_{trans} = melting temperature, T_m) or amorphous (T_{trans} = glass transition temperature, T_g) regions within the polymer that allow molecular movement above a certain temperature and fixation below that same temperature (i.e. transition temperature, T_{trans}). At $T>T_{trans}$, a temporary shape can be formed with the application of stress, after which the shape may be fixed by cooling to $T<T_{trans}$. Defining the permanent shape, "netpoints" are chemical or physical cross-links between polymer chains. Thus, the original shape can be retrieved by heating to $T>T_{trans}$.

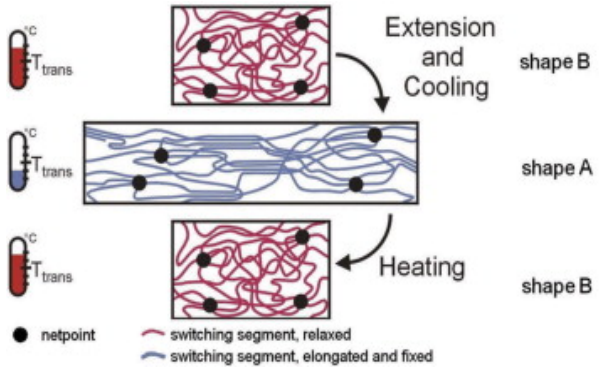

Figure 2. Mechanism of the thermally induced shape-memory effect for a semi-crystalline thermoset.[2]

When cross-linked, PCL-DA is particularly useful due to the covalent cross-links, or "netpoints," and its semi-crystallinity (i.e. "switching segments") giving rise to shape memory ability. Additionally, the T_m (T_{trans}) is well defined, in a clinically relevant range of 43-60°C.[15] Notably, SMP scaffold properties are readily controlled as they are established prior to implantation, and the scaffold will not undergo shrinkage within the defect. In this way, this scaffold strategy overcomes the limitations of many *in-situ* forming fillers and scaffolds.

Tissue Engineering

Given the limitations associated with treating CMF defects with autografts, a tissue engineering approach based on a synthetic scaffold could greatly improve healing outcomes (**Figure 3**). Tissue engineering generally refers to the combined use of a scaffold, cells, and optionally bioactive molecules to restore, maintain, or improve damaged tissues.[16] In the specific case of scaffolds useful to treat irregularly shaped CMF bone defects, several key functional requirements must be achieved. First, as noted above, the scaffold must form close contact with adjacent bone tissue to permit osseointegration while avoiding brittle mechanical properties so as to not undergo post-surgical fracture.[17] Second, the scaffold should permit cell migration, nutrient diffusion and neotissue deposition.[18] Currently, no single scaffold or on-the-market bone substitute intrinsically provides all of these crucial properties.[4]

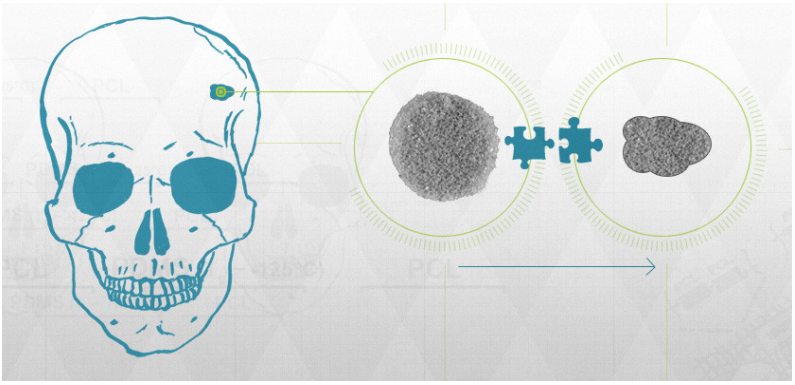

Figure 3. Schematic showing porous scaffolds to heal CMF defects.[1]

In order to fill the irregular bone defect, scaffolds which cure *in situ* are often used or proposed. For instance, synthetic bone substitutes (e.g. putties and cements prepared with and without ceramic or glass ceramic fillers) have been investigated. Unfortunately, these suffer from major limitations including: extreme exothermic cure (up to ~90 ºC), slow setting times (with "fast sets" requiring ~24 hours), low pore interconnectivity, lack of degradation (leading to poor healing), and brittle mechanical properties (leading to fracture during surgical contouring as well

as post-surgery).[19-20] Hydrogels have also been considered, but do not demonstrate sufficient mechanical properties and often exhibit variable local curing times leading to poor adhesion to the defect edges.[18, 21] Furthermore, cytotoxic reagents used in synthesis of the hydrogel (e.g. monomers, crosslinkers, and catalysts) may be problematic for *in situ* cure scenarios.[21]

Other conventional techniques for polymer-based scaffold fabrication include particulate leaching[22-23], phase separation[24-25], and gas foaming.[26-27] Many of these methods offer high tunability and excellent control over the scaffolds' physical properties (e.g. pore size, pore interconnectivity and porosity, modulus, and bioactivity) necessary for enhanced bone regeneration. However, precise control of the scaffold 3D geometry to match the defect contours is generally confined to the shape of the fabrication mold and post-fabrication contouring which is particularly challenging for brittle materials such as most ceramics.[28-31] Furthermore, computer-aided solid free-form fabrication (SFF) techniques may generate complex scaffold shapes but are costly and time-consuming.[32-33]

Towards improving CMF defect treatment, we have previously reported a porous, SMP scaffold based on PCL-DA that, after exposing to warm saline, can be press-fitted into irregular defects.[34] The material, as a nonporous solid, has potential use for biomedical applications such as minimally invasive cardiovascular devices and custom-fitted biodegradable fixation devices.[35]

Prior to deployment into the defect, the SMP scaffold would be briefly treated with moderately warm saline (~55 °C for ~30 seconds) such that it becomes malleable, allowing a "generically-prepared" cylindrical scaffold to be hand pressed into the irregular defect. Within only ~5 min after placement, the scaffold rigidizes as it cools and locks in the new temporary shape within the defect. Finally, since not mechanically brittle (in contrast to putties and cements), the scaffolds may be further surgically contoured and are also resistant to cracking post-surgery.[36] This

solution satisfies the key requirements for CMF defect repair, including: the ability to be contoured to "fit" irregular defects, a highly porous environment for osteoconduction, bioactivity (i.e. bone-bonding ability), temporary mechanical strength, and controlled biodegradation. As described in this work, by tuning PCL-DA *n*, key physical properties of the PCL-DA SMP self-fitting scaffolds could be tuned to enhance their potential to fulfill these requirements and thus improve their capacity to heal irregular bone defects.

CHAPTER II

MATERIALS AND METHODS

Materials

ε-Caprolactone monomer, stannous 2-ethylhexanoate, triethylamine (Et_3N), acryloyl chloride, 4-dimethylaminopyridine (DMAP), 2,2-dimethoxy-2-phenylacetophenone (DMP), 1-vinyl-2-pyrrolidinone (NVP), potassium carbonate (K_2CO_3), sodium hydroxide (NaOH), ethylene glycol, and solvents were obtained from Sigma-Aldrich. Anhydrous magnesium sulfate ($MgSO_4$) was obtained from Fisher. Reagent-grade CH_2Cl_2 and NMR-grade $CDCl_3$ were dried over 4 Å molecular sieves prior to use.

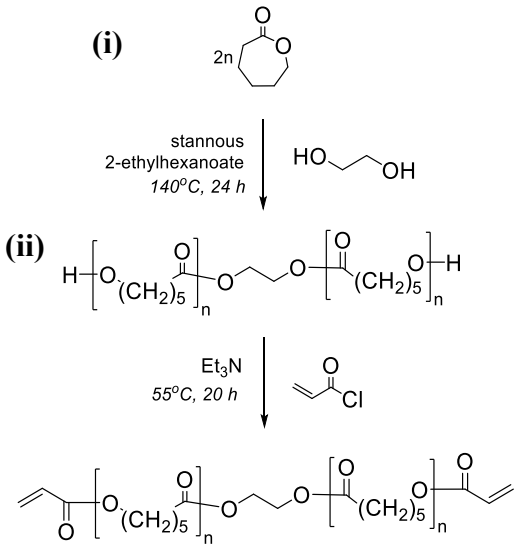

Figure 4. Synthetic strategy of **(i)** PCL via ring opening polymerization and subsequent **(ii)** acrylation of PCL-diol to yield PCL diacrylate.

Material Synthesis

PCL_{2n}-diol was synthesized by the ring opening polymerization of ε-caprolactone in the presence of ethylene glycol initiator and stannous 2-ethylhexanoate catalyst (**Figure 4i)**. The degree of polymerization (*n*) was controlled by the ratio of ε-caprolactone to ethylene glycol. The terminal hydroxyl groups were subsequently reacted with acryloyl chloride to produce photosensitive acrylate (OAc) groups (**Figure 4ii**). The degree of polymerization (*n*) was confirmed with ^{1}H Nuclear Magnetic Resonance (NMR) spectroscopy using a Mercury 300 MHz spectrometer operating in the Fourier transform (FT) mode and using $CDCl_3$ as the standard.

Scaffold Fabrication

Porous scaffolds (*n = 20, 40, 60,* and *70*) were fabricated by photocuring a precursor solution of the designated macromer around a fused salt template.[34, 36] To prepare the fused salt template, a 425μm sieve was used to obtain sodium chloride (NaCl) particles of uniform diameter (459 ± 69 μm). De-ionized water (7.5 wt%) was then added in four equal portions to 1.8 g of the NaCl in a 3 mL glass vial. The salt was mixed after each addition to ensure even water distribution among particles. Centrifugation (4000 rpm for 15 minutes) and vacuum drying resulted in fusion of the salt into the final template. A macromer solution of PCL-DA in DCM (0.15 g/mL) was prepared with 15 vol% photoinitiator (10 wt% DMP in NVP). The solution was added to the prepared fused salt template (~0.6 mL/vial) and centrifuged (2500 rpm for 10 minutes) in order to facilitate infiltration of the macromer solution into the template. The vial was then exposed to UV light (6 mW cm^2, 365 nm) for 3 minutes to initiate cross-linking. After air-drying overnight, the scaffold was removed from the vial and placed in a solution of water and ethanol (50:50) for 4 days to dissolve and remove the salt. Lastly, the scaffolds were annealed at 85°C, for 1h, *in vacuo*.

Characterization

Thermal Properties

Differential Scanning Calorimetry (DSC, TA Instruments Q100) was used to determine percent crystallinity. PCL-DA macromer samples (~12 mg, N = 3) in hermetic pans were heated from -80 ºC to 80 ºC at 5 ºC/min for two cycles. Data was collected from the second heating cycle. Scaffold specimens (~8 mg, N=3) in hermetically sealed pans were similarly heated from 0 ºC to 80 ºC at a heating rate of 5 ºC/min. From the endothermic PCL melting peak, enthalpy change (ΔH_m) was measured. Percent crystallinity (% χ_c) was calculated via **Equation 1**.

Equation 1. $$\%\chi c = \frac{\Delta H_m}{\Delta H_m^0} \times 100$$

ΔH_m was calculated by integration of the area of the melting peak, and ΔH^0_m is the enthalpy of fusion of 100% crystalline PCL (139.5 J/g).[15]

Mechanical Properties

Compression tests of cylindrical foams (6 mm diameter x 5 mm height) were performed using an Instron 3340 at room temperature. Specimens were subjected to a constant compressive strain rate (1.5 mm/min) up to 85% strain. Compressive modulus (*E*) was determined by calculating the slope of the initial linear portion of the stress-strain curve**.** Compressive strength was determined as the stress at 85% strain.

Degradation

Degradation rate was sacrificially measured via mass loss under accelerated, basic conditions (37°C in 1M NaOH solution) at 24 h, 72 h, 168 h, and 264 h. Each scaffold (6mm diameter x 5 mm height, N=3) was immersed in 20 mL of 1M NaOH in a sealed centrifuge tube and maintained at 37 ºC in a temperature controlled water bath. After the assigned hours passed,

specimens were removed, blotted with a Kim Wipe and dried *in vacuo* overnight. The weight of the dried specimen was recorded.

Porosity

Interconnected porosity was confirmed and pore size was determined via scanning electron microscopy (SEM). Cross-sections of each scaffold were subjected to an Au-Pt coating (~4 nm) and examined by SEM (JEOL 6400) at accelerated voltage of 15 kV. Percent porosity was calculated using **Equation 2**, in which "$\text{density}_{\text{SMP scaffold}}$" was gravimetrically determined and "$\text{density}_{\text{solid SMP}}$" is the density of the analogous solid SMP.

Equation 2. $$\%porosity = \frac{density_{solid\ SMP} - density_{SMP\ scaffold}}{density_{solid\ SMP}} \times 100$$

CHAPTER III

RESULTS

Thermal Properties

Upon crosslinking to form a porous scaffold, trends in crystallinity vary versus those of the uncrosslinked macromer. Results indicated that the *n = 20* scaffolds were significantly less crystalline when compared to the other three scaffold compositions whose crystallinity were statistically similar (**Figure 5**). Importantly, all compositions showed sufficient crystallinity (~30%) to maintain shape memory since the crystalline segments act as the switching segments.[37]

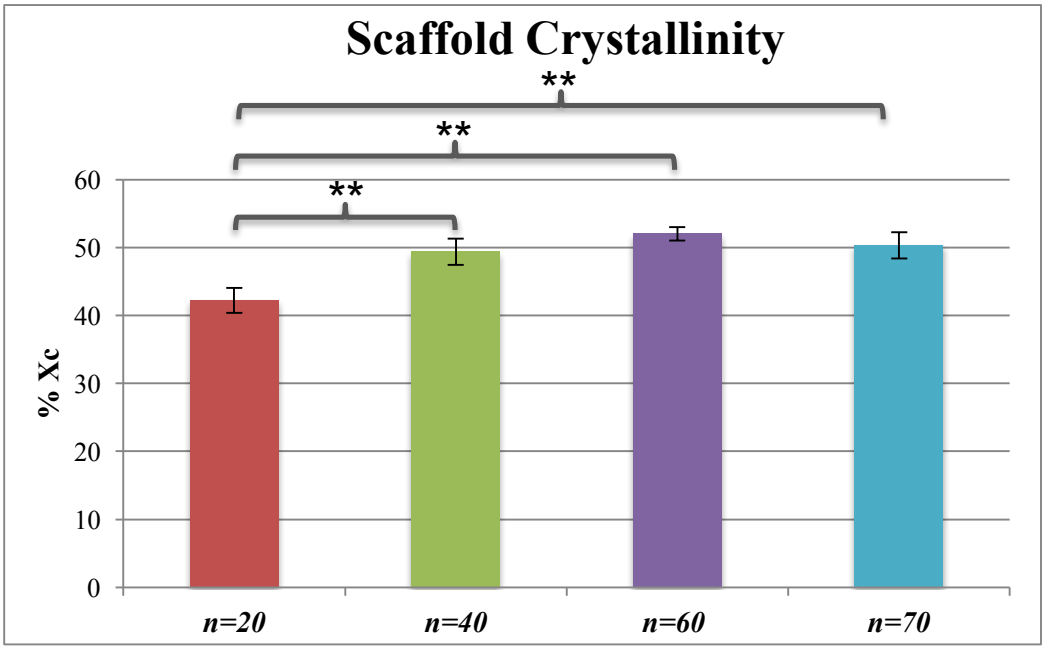

Figure 5. % Crystallinity of scaffolds. (** indicates p<0.01)

Results from DSC on the macromer indicated that *n = 60* was significantly more crystalline than *n = 40* or *n = 70* but similar to *n = 20* (**Figure 6)**. The data indicates that, in bulk form, PCL-DA macromer crystallinity is dependent on the value of *n* (i.e. chain length). Thus, chain length determines the extent to which PCL lamellae are able to form in the uncrosslinked PCL polymer.

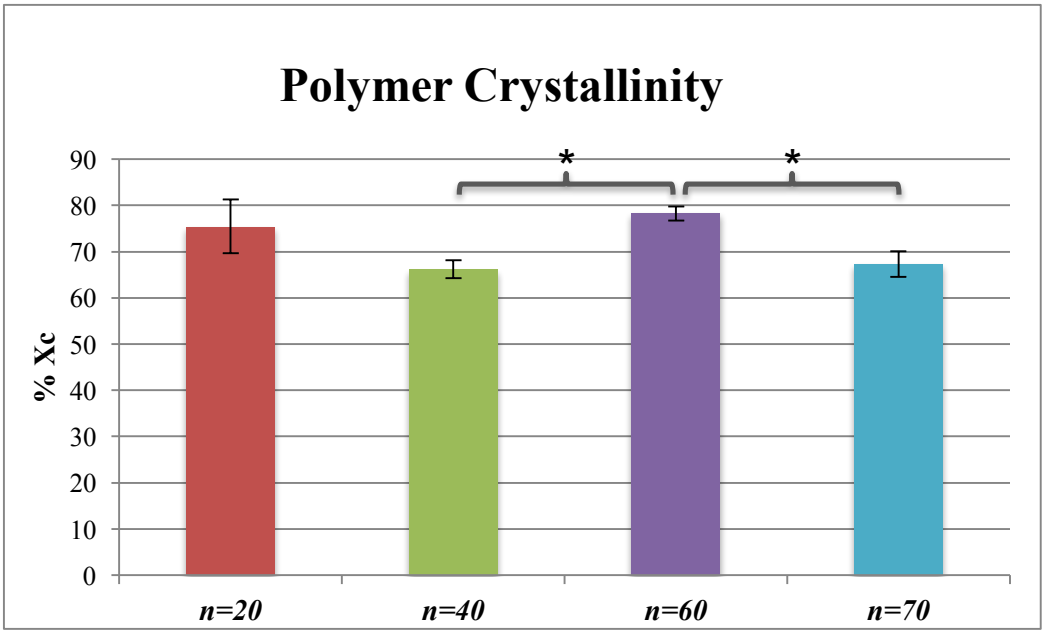

Figure 6. % crystallinity of PCL-DA macromers (* indicates $p<0.05$).

Mechanical Properties

For crosslinked PCL-DA porous scaffolds, compression tests indicated that *n = 20* was significantly less strong when compared to *n = 40* and *n = 60* (**Figure 7**). Several different trends in mechanical properties can occur in polymers due to different physical properties. In covalently cross-linked networks, a decrease in degree of polymerization (*n*) produces a higher cross-link density, generally resulting in an increase in modulus and strength unless the system becomes very brittle.[38] Furthermore, higher % crystallinity tends to correspond to an increase in modulus and strength due to significant intermolecular bonding in the crystalline phase.[39] **Figure 7** and **Figure 8**, respectively, show the strength and modulus of the different SMP scaffold compositions. While

compressive modulus was statistically similar for all scaffolds, the compressive strength was lowest for *n = 20*. This decrease in strength may be due to the reduced crystallinity of the scaffold.

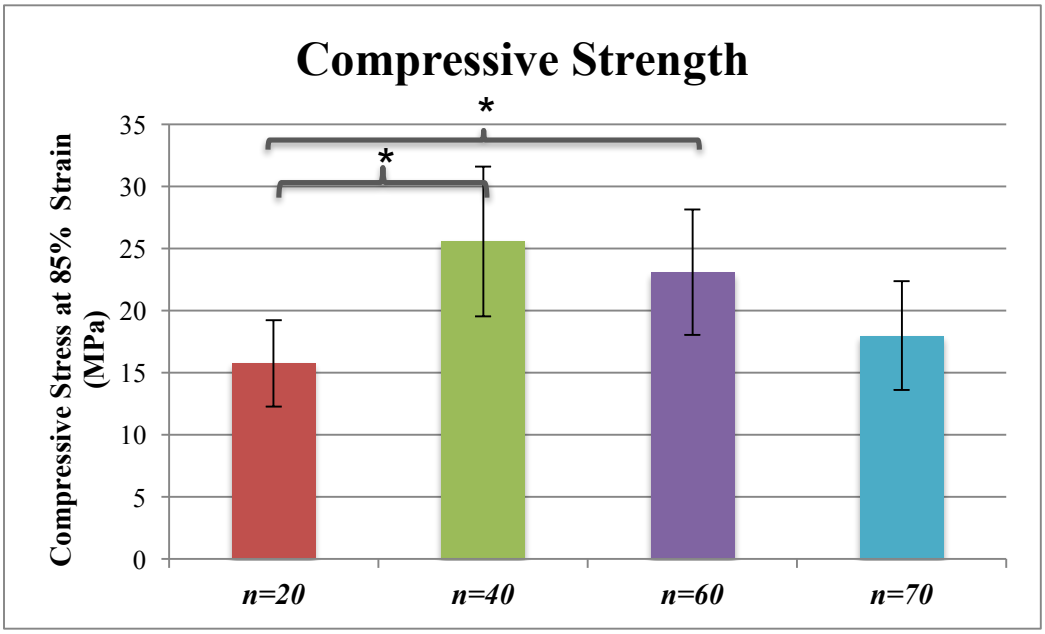

Figure 7. Compressive strength of scaffolds. (* indicates $p<0.05$).

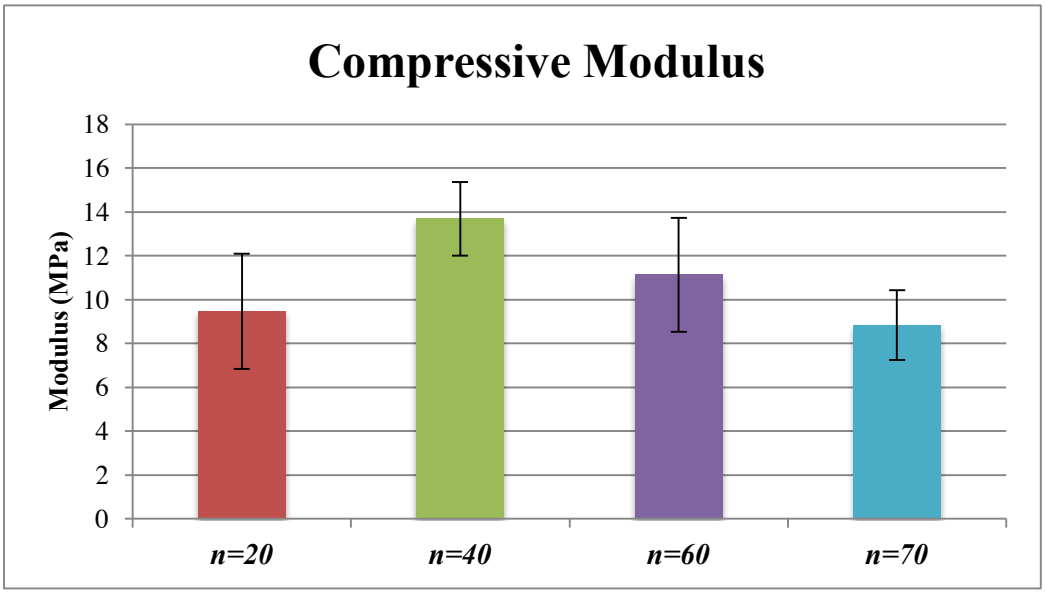

Figure 8. Compressive modulus of scaffolds.

Degradation

Results indicated that n = 20 scaffolds degraded significantly faster than the other compositions (**Figure 9**). Typically, a more highly crosslinked network would diminish water infiltration and reduce the rate of degradation. Thus, we attribute the faster degradation of $n = 20$ to its overall lower % crystallinity which is also known to increase degradation rates by inhibiting water infiltration.

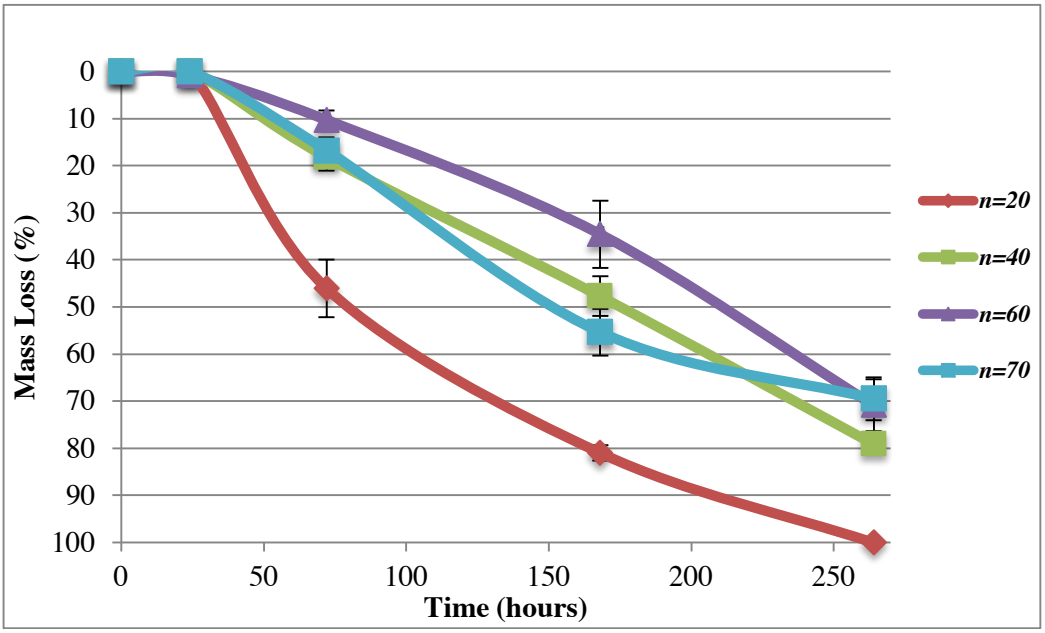

Figure 9. Scaffold degradation

During degradation, the appearance of the scaffolds was also visually observed (**Figure 10**). At the last time point (264 h), $n = 20$ scaffolds were completely disintegrated.

Figure 10. Images of scaffolds during degradation.

Porosity

SEM images revealed that SMP scaffolds contained interconnected pores of uniform pore size (**Figure 11**). These images indicate that in every composition, pores were of sufficient size (>200 μm) to allow cell infiltration to facilitate new bone growth and nutrient and waste transportation (**Table 1**). Thus, the utilized fabrication method involving solvent-casting particulate leaching allowed facile control of the pore size and uniformity which is essential to achieve scaffold characteristics conducive to bone healing.

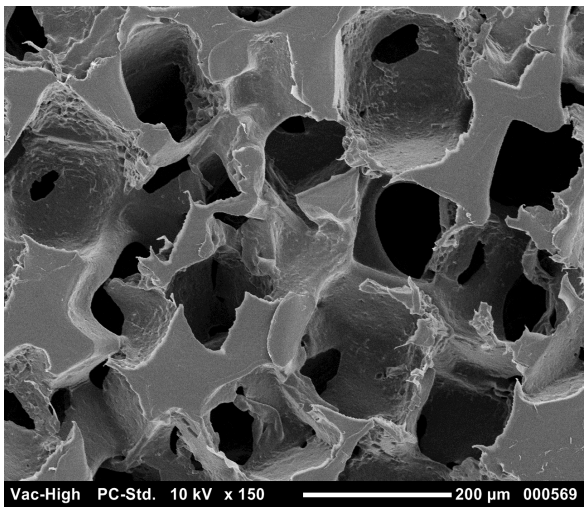

Figure 11. SEM image illustrating interconnected porosity of SMP scaffold.

Table 1. Pore size and % porosity (** indicates p<0.01).

Composition	*n = 20*	*n = 40*	*n = 60*	*n = 70*
Avg. Pore Size (µm)	234 ± 31.2	206 ± 47.2 **	234 ± 27.2	243 ± 28.6

Using a gravimetric technique, pore size (**Table 1**) and % porosity (**Figure 12**) of SMP scaffolds was quantitatively determined. Due to the use of the same salt size and amount of water added to form the fused salt template, all scaffolds had similar pore sizes. The slightly smaller pore size of *n = 40* may be attributed to its higher crystallinity that may have led to greater shrinking during annealing. Due to the slightly smaller pore size, the % porosity of *n = 40* scaffolds was also statistically, but not substantially, decreased when compared to all other compositions (**Figure 12**). Its lower % porosity may have also contributed to the increased strength and modulus of the *n = 40* scaffold as this is a generally observed relationship.[40]

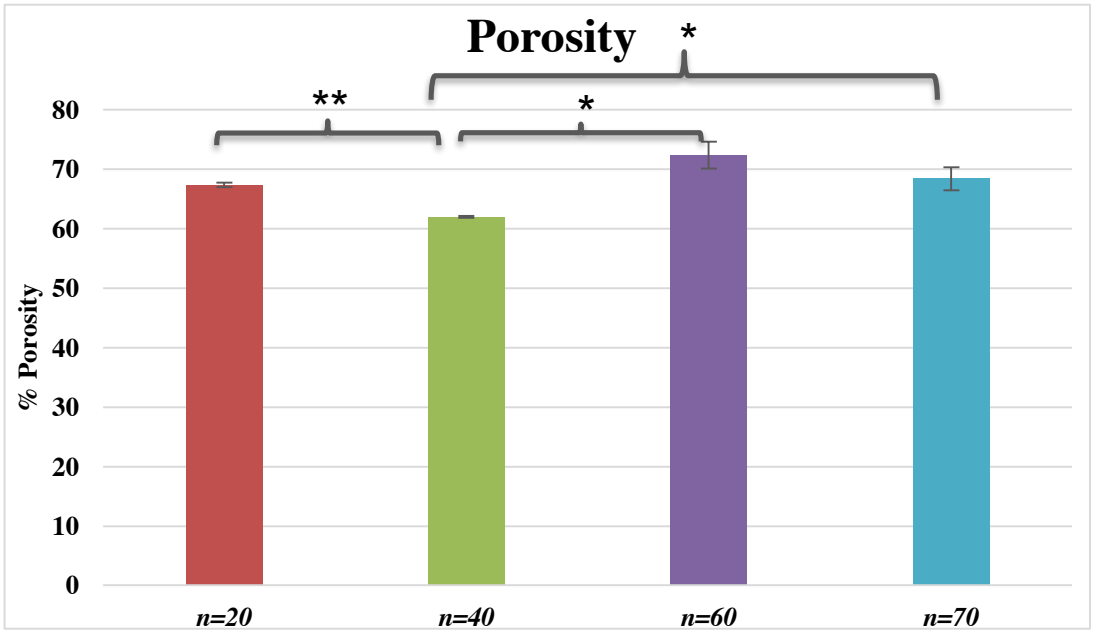

Figure 12. % porosity of scaffolds

Statistical Analysis

Results are given as mean ± standard deviation (N = 3). Sample means were compared using ANOVA followed by a Student's t-Test with $p<0.05$ indicating significant difference.

CHAPTER IV

CONCLUSION

In this work, SMP scaffolds were prepared using PCL-DA macromers with systematically tuned degrees of polymerization (*n = 20, 40, 60* and *70*). Scaffolds were prepared using a solvent-casting particulate leaching technique in which a solution containing the PCL-DA macromer was UV-cured around a fused salt template. The impact of PCL-DA degree of polymerization on % crystallinity, mechanical properties, degradation rate, pore size, and % porosity were evaluated.

All SMP scaffold compositions were found to maintain sufficient crystallinity (~30%) in order to exhibit shape memory effect as the crystalline domains effectively act as the "switching segments" of the PCL-DA SMP. However, *n = 20* scaffolds were found to have reduced crystallinity when compared to the other compositions likely attributing to the increased degradation rate of the *n = 20*.

For the PCL-DA scaffolds, % crystallinity, porosity, and degree of polymerization had a greater influence on mechanical properties than the cross-link density resulting in a low compressive strength for *n = 20* scaffolds. The *n = 40* scaffolds generally showed improved mechanical properties, potentially due to the balance in enhanced crystallinity and moderate crosslinking density. The *n = 40* scaffolds also showed smaller pore size and lower % porosity, perhaps correlating to the slightly more robust mechanical properties.

In future work, an understanding of the effects of PCL-DA degree of polymerization (*n*) on key scaffold properties will be useful to further broaden scaffold properties. Our group is also investigating the effects of adding thermoplastic PLLA into the cross-linked network of PCL-DA

as a semi-interpenetrating network (semi-IPN).[15] Thorough knowledge of how the cross-link density of the PCL-DA network affects properties will aide this development.

REFERENCES

1. Repair of Bone Defects with Shape Memory Polymers. http://grunlanlab.tamu.edu/.

2. Marc Behl, A. L., Shape-memory polymers. *Materials Today* **2007,** *10* (4), 20-28.

3. T., E. In *Basic Science of Bone Graft Substitutes* Annual Meeting of the Orthopaedic Trauma Association., Salt Lake City, UT, Salt Lake City, UT, 2003.

4. Szpalski, C., Barr, J., Wetterau, M., Saadeh, P.B., & Warren, S.M., Cranial bone defects: current and future stretegies. *Neurosurgical Focus* **2010**.

5. Kumar, K. V., Singla, N. K., Gowda, M. E., Kumar, D., & Legha, V. S. , Current Concepts in Restoring Acquired Cranial Defects. *The Journal of Indian Prosthodontic Society* **2014**, p. 14-17.

6. Quereshy FA, D. H., El SA, Horan MP, Dhaliwal SS., Resorbable screw fixation for cortical onlay bone grafting: a pilot study with preliminary results. *J Oral Maxillofac Surg* **2010,** *68* (10), 2497-2502.

7. H. M. Wache, D. J. T., A. Hentrich, M. H. Wagner, Development of a polymer stent with shape memory effect as a drug delivery system. *Journal of Materials Science: Materials in Medicine* **2003,** *14* (2), 109–112.

8. Lendlein, A., Langer, R., Biodegradable, Elastic Shape-Memory Polymers for Potential Biomedical Applications. *Science* **2002,** *296* (5573), 1673-1676.

9. Lendlein, A.; Langer, R., Biodegradable, elastic shape-memory polymers for potential biomedical applications. *Science* **2002,** *296* (5573), 1673-1676.

10. Yakacki, C. M.; Shandas, R.; Safranski, D.; Ortega, A. M.; Sassaman, K.; Gall, K., Strong, Tailored, Biocompatible Shape-Memory Polymer Networks. *Adv. Funct. Mater.* **2008,** *18* (16), 2428-2435.

11. Xie, T., Tunable polymer multi-shape memory effect. *Nature* **2010,** *464* (7286), 267-270.

12. Lendlein, A.; Jiang, H.; Junger, O.; Langer, R., Light-induced shape-memory polymers. *Nature* **2005,** *434* (7035), 879-882.

13. Kumpfer, J. R.; Rowan, S. J., Thermo-, Photo-, and Chemo-Responsive Shape-Memory Properties from Photo-Cross-Linked Metallo-Supramolecular Polymers. *J. Am. Chem. Soc.* **2011,** *133* (32), 12866-12874.

14. Buckley, P. R.; McKinley, G. H.; Wilson, T. S.; Small, W.; Benett, W. J.; Bearinger, J. P.; McElfresh, M. W.; Maitland, D. J., Inductively Heated Shape Memory Polymer for the Magnetic Actuation of Medical Devices. *IEEE Trans. Biomed. Eng.* **2006,** *53* (10), 2075-2083.

15. Lindsay N. Woodard, V. M. P., Kevin T. Kmetz, Melissa A. Grunlan, PCL-PLLA Semi-IPN Shape Memory Polymers (SMPs): Degradation and Mechanical Properties. *Macromolecular Rapid Communications* **2016,** *37* (23), 1972-1977.

16. Tissue Engineering and Regenerative Medicine. (accessed March 29).

17. Alsberg, E., Hill, E. & Mooney, D. , Craniofacial tissue engineering. *Crit. Rev. Oral. Biol. M.* **2011,** *12*, 64-75.

18. Prieto, E. M., Page, J. M., Harmata, A. J. & Guelcher, S. A. , Injectable foams for regenerative medicine. . *WIREs Nanomed. Nanobiotechnol.* **2014,** *6*, 136-154.

19. Shah, A. M., Jung, H. & Skirboll, S. , Materials used in cranioplasty: a history and analysis. *Neurosurg. Focus.* **2014** *36* (18).

20. Manson, P. N., Crawley, W. A. & Hoopes, J. E. , Frontal Cranioplasty: Risk Factors and Choice of Cranial Vault Reconstructive Material. *Plast. Reconstr. Surg.* **1986,** *77*, 888-900.

21. Drury, J. L. M., D. J., Hydrogels for tissue engineering: scaffold design variables and applications. *Biomaterials* **2003,** *24*, 4337-4351.

22. Mikos, A. G.; Thorsen, A. J.; Czerwonka, L. A.; Bao, Y.; Langer, R.; Winslow, D. N.; Vacanti, J. P., Preparation and characterization of poly(l-lactic acid) foams. *Polymer* **1994,** *35* (5), 1068-1077.

23. Lu, L.; Peter, S. J.; D. Lyman, M.; Lai, H.-L.; Leite, S. M.; Tamada, J. A.; Uyama, S.; Vacanti, J. P.; Robert, L.; Mikos, A. G., In vitro and in vivo degradation of porous poly(dl-lactic-co-glycolic acid) foams. *Biomaterials* **2000,** *21* (18), 1837-1845.

24. Nam, Y. S.; Park, T. G., Porous biodegradable polymeric scaffolds prepared by thermally induced phase separation. *J. Biomed. Mater. Res.* **1999,** *47* (1), 8-17.

25. Smith, L. A.; Ma, P. X., Nano-fibrous scaffolds for tissue engineering. *Colloids Surf., B* **2004,** *39* (3), 125-131.

26. Nazarov, R.; Jin, H.-J.; Kaplan, D. L., Porous 3-D Scaffolds from Regenerated Silk Fibroin. *Biomacromolecules* **2004,** *5* (3), 718-726.

27. Mathieu, L. M.; Mueller, T. L.; Bourban, P.-E.; Pioletti, D. P.; Müller, R.; Månson, J.-A. E., Architecture and properties of anisotropic polymer composite scaffolds for bone tissue engineering. *Biomaterials* **2006,** *27* (6), 905-916.

28. Giannoudis, P. V.; Dinopoulos, H.; Tsiridis, E., Bone substitutes: An update. *Injury* **2005,** *36* (3, Supplement), S20-S27.

29. Takahashi, Y.; Yamamoto, M.; Tabata, Y., Enhanced osteoinduction by controlled release of bone morphogenetic protein-2 from biodegradable sponge composed of gelatin and β-tricalcium phosphate. *Biomaterials* **2005,** *26* (23), 4856-4865.

30. Ren, J.; Zhao, P.; Ren, T.; Gu, S.; Pan, K., Poly (d,l-lactide)/nano-hydroxyapatite composite scaffolds for bone tissue engineering and biocompatibility evaluation. *Journal of Materials Science: Materials in Medicine* **2008,** *19* (3), 1075-1082.

31. Puértolas, J. A.; Vadillo, J. L.; Sánchez-Salcedo, S.; Nieto, A.; Gómez-Barrena, E.; Vallet-Regí, M., Compression behaviour of biphasic calcium phosphate and biphasic calcium phosphate–agarose scaffolds for bone regeneration. *Acta Biomaterialia* **2011,** *7* (2), 841-847.

32. Hollister, S. J., Porous scaffold design for tissue engineering. *Nat. Mater.* **2005,** *4* (7), 518-524.

33. Sachlos, E.; Czernuszka, J., Making tissue engineering scaffolds work. Review: the application of solid freeform fabrication technology to the production of tissue engineering scaffolds. *Eur. Cell Mater.* **2003,** (5), 29-39.

34. Zhang, D., George, O. J., Petersen, K. M., Jimenez-Vergara, A. C., Hahn, M. S., & Grunlan, M. A. , A bioactive “self-fitting” shape memory polymer scaffold with potential to treat cranio-maxillo facial bone defects. *Acta Biomaterialia* **2014**, p. 4597-4605.

35. Agrawal, C. M., & Ray, R. B., Biodegradable polymeric scaffolds for musculoskeletal tissue engineering. *Journal of Biomedical Materials Research* **2001,** *55* (2), 141-150.

36. Lindsay N. Nail, D. Z., Jessica L. Reinhard, Melissa A. Grunlan, Fabrication of a Bioactive, PCL-based "Self-fitting" Shape Memory Polymer Scaffold. *Journal of Visualized Experiments* **2015,** (104).

37. Cody Alan Schoener, C. B. W., Ranjini Murthya and Melissa Ann Grunlan, Shape memory polymers with silicon-containing segments. *Journal of Materials Chemistry* **2010,** *20* (9), 1787-1793.

38. Sperling, L. H., *Introduction to Physical Polymer Science*. John Wiley & Sons, Inc.: New York, NY, 2001.

39. Kantesh Balani, V. V., Arvindd Agarwal, Roger Narayan, Physical, Thermal, and Mechanical Properties of Polymers. In *Biosurfaces: A Materials Science and Engineering Perspective* John Wiley & Sons, Inc: Hoboken, NJ, USA, 2014.

40. Ikeda, R., Hiroyuki Fujioka, Issei Nagura, Takeshi Kokubu, Narikazu Toyokawa, Atsuyuki Inui, Takeshi Makino, Hiroaki Kaneko, Minoru Doita, and Masahiro Kurosaka, The effect of porosity and mechanical property of a synthetic polymer scaffold on repair of osteochondral defects. *International Orthopaedics* **2008,** *33* (3), 821-28.